



ARTICLE

Intramuscular injection of sotagliflozin promotes neovascularization in diabetic mice through enhancing skeletal muscle cells paracrine function

Lai-liu Luo^{1,2}, Jing-xuan Han^{1,2}, Shou-rong Wu^{1,2,3} and Vivi Kasim^{1,2,3}

Diabetes mellitus is associated with series of macrovascular and microvascular pathological changes that cause a wide range of complications. Diabetic patients are highly susceptible to hindlimb ischemia (HLI), which remains incurable. Evidence shows that skeletal muscle cells secrete a number of angiogenic factors to promote neovascularization and restore blood perfusion, this paracrine function is crucial for therapeutic angiogenesis in diabetic HLI. In this study we investigated whether sotagliflozin, an anti-hyperglycemia SGLT2 inhibitor, exerted therapeutic angiogenesis effects in diabetic HLI in vitro and in vivo. In C2C12 skeletal muscle cells, we showed that high glucose (HG, 25 mM) under hypoxia markedly inhibited cell viability, proliferation and migration potentials, which were dose-dependently reversed by pretreatment with sotagliflozin (5–20 μ M). Sotagliflozin pretreatment enhanced expression levels of angiogenic factors HIF-1 α , VEGF-A and PDGF-BB in HG-treated C2C12 cells under hypoxia as well as secreted amounts of VEGF-A and PDGF-BB in the medium; pretreatment with the HIF-1 α inhibitor 2-methoxyestradiol (2-ME2, 10 μ M) or HIF-1 α knockdown abrogated sotagliflozin-induced increases in VEGF-A and PDGF-BB expression, as well as sotagliflozin-stimulated cell proliferation and migration potentials. Furthermore, the conditioned media from sotagliflozin-treated C2C12 cells in HG medium enhanced the migration and proliferation capabilities of vascular endothelial and smooth muscle cells, two types of cells necessary for forming functional blood vessels. In vivo study was conducted in diabetic mice subjected to excising the femoral artery of the left limb. After the surgery, sotagliflozin (10 mg/kg) was directly injected into gastrocnemius muscle of the left hindlimb once every 3 days for 3 weeks. We showed that intramuscular injection of sotagliflozin effectively promoted the formation of functional blood vessels, leading to significant recovery of blood perfusion in diabetic HLI mice. Together, our results highlight a new indication of SGLT2 inhibitor sotagliflozin as a potential therapeutic angiogenesis agent for diabetic HLI.

Keywords: diabetes; hindlimb ischemia; sotagliflozin; angiogenesis; HIF-1 α ; skeletal muscle cells; vascular endothelial cells; smooth muscle cells

Acta Pharmacologica Sinica (2022) 43:2636–2650; <https://doi.org/10.1038/s41401-022-00889-4>

INTRODUCTION

Diabetes mellitus is a lifelong metabolic disease characterized by chronic hyperglycemia [1]. International Diabetes Federation estimated that 1 in 11 adults aged 20–79 years (415 million adults) had diabetes mellitus globally in 2015. Furthermore, this number is projected to rise to 642 million by 2040, as the trend keeps increasing [2]. Despite the tremendous efforts put into prolonging the lives of patients with diabetic mellitus, diabetes has remained as the fifth leading cause of death worldwide and has directly resulted in 1.6 million deaths [3]. In chronic conditions, diabetes can lead to long-term damage, dysfunction, and failure of different organs, especially eyes, kidneys, nerves, heart, and blood vessels [4]. Unfortunately, until now, no complete cure for diabetes has been found [5, 6].

Vascular complications are the leading causes of morbidity and mortality in diabetic patients [7]. Diabetic hindlimb ischemia (HLI)

stands for the pathological changes of blood vessels and nerves in the feet of diabetic patients, resulting in insufficient blood supply, especially to the lower extremity [8]. In severe cases, HLI could lead to tissue necrosis, amputation and even death. Indeed, diabetes has become the main cause of non-traumatic amputation [9].

Currently, there have been limited advances in therapies for diabetic HLI. Revascularization approach is largely inappropriate for diabetic HLI patients due to larger wound surface areas and higher rates of relapse compared to non-diabetic patients. Furthermore, patients with critical limb ischemia, the most severe stage of HLI whose risk is even significantly higher in diabetic patients compared to non-diabetic patients, could not receive revascularization treatments due to severe damages in their vessels. For these “no-option” patients, amputation is frequently inevitable to prevent the generation of other complications

¹Key Laboratory for Biorheological Science and Technology of Ministry of Education, College of Bioengineering, Chongqing University, Chongqing 400044, China; ²The 111 Project Laboratory of Biomechanics and Tissue Repair, College of Bioengineering, Chongqing University, Chongqing 400044, China and ³State and Local Joint Engineering Laboratory for Vascular Implants, College of Bioengineering, Chongqing University, Chongqing 400044, China

Correspondence: Shou-rong Wu (shourongwu@cqu.edu.cn) or Vivi Kasim (vivikasim@cqu.edu.cn)

These authors contributed equally: Lai-liu Luo, Jing-xuan Han

Received: 20 November 2021 Accepted: 13 February 2022

Published online: 15 March 2022

[10, 11]. For approximately two decades, therapeutic angiogenesis is one of the most studied and regarded as an effective promising strategy for HLI disease, especially for nonrevascularizable patients [12]. However, hyperglycemia disrupts internal angiogenic potential, causing ineffective induction of angiogenesis to yield a successful therapy in diabetic HLI patients.

Skeletal muscle cells, the largest paracrine and endocrine organ, is an attractive target for therapeutic angiogenesis, as they could secrete paracrine and autocrine signals, including vascular endothelial growth factor-A (VEGF-A), platelet-derived growth factor-BB (PDGF-BB), fibroblast growth factor 2 (FGF2), and heme oxygenase-1 (HO-1) [13–15]. These factors could positively influence vascular endothelial and smooth muscle cells, and subsequently enhance neoangiogenesis [13, 14, 16, 17]. Vascular endothelial cells, which initiates angiogenesis by forming the inner vessel tubes, and smooth muscle cells, which cover the vessel tubes formed by vascular endothelial cells, are two fundamental cells forming functional and mature vessels [18]. Meanwhile, growing evidences from pre-clinical and clinical studies have implicated alterations in hypoxia-inducible factor 1 (HIF-1 α) levels, which regulates various angiogenic factors including VEGF-A and PDGF-BB, in the abrogation of pro-angiogenic pathways [19], and that stabilization of skeletal muscle cells HIF-1 α might benefit angiogenesis [20, 21]. Furthermore, our previous studies have shown that targeting skeletal muscle cells and improving their paracrine function could serve as a potential therapeutic strategy for HLI [17, 22, 23].

Sotagliflozin, a dual inhibitor of sodium-glucose co-transporter-2 (SGLT2) and sodium-glucose co-transporter-1, is an anti-hyperglycemic drug that has been approved by the European Medicines Agency [24]. Recent study showed that sotagliflozin could significantly lower the total number of deaths from cardiovascular causes in patients with diabetes and chronic kidney disease [25, 26]. However, whether sotagliflozin could exert therapeutic angiogenesis effects in diabetic HLI is still unknown. Here we showed that SGLT2 inhibitor sotagliflozin could significantly enhance the viability and paracrine function of skeletal muscle cells, which subsequently promote neovascularization in diabetic HLI mice.

MATERIALS AND METHODS

Chemicals

Sotagliflozin (purity $\geq 99\%$) was purchased from Meilunbio (Shenyang, China). Mannitol (purity $\geq 99\%$) was purchased from Macklin Biochemical (Shanghai, China). Streptozocin (STZ; purity $\geq 75\%$) was purchased from Sigma-Aldrich (St Louis, MO, USA).

Cell lines and cell culture

C2C12, HUVECs, and MOVAS cell lines were purchased from the American Type Culture Collection. Cells were cultured with Dulbecco's modified Eagle's medium (DMEM; Gibco, Life Technologies, Grand Island, NY, USA) with 10% fetal bovine serum (FBS; Biological Industries, Beit Haemek, Israel) and 1% penicillin/streptomycin (Gibco) in a humidified incubator (37 °C, 5% CO₂). Prior to use in cell culture experiments, C2C12 cells were differentiated into myotubes by culturing them in DMEM with 2% horse serum (Biological Industries) and 1% penicillin/streptomycin for 5 days [27]. Normal glucose condition was obtained by culturing the cells in DMEM with a final glucose concentration of 7.5 mM, while hyperglycemic condition was obtained by culturing the cells in DMEM with a final glucose concentration of 25 mM. High osmotic group was established by culturing the cells in normal glucose condition with 17.5 mM mannitol (final concentration). Cells were then exposed to hypoxia in a hypoxia chamber (Anaeropouch Box, 0.1% O₂, Mitsubishi Gas Chemical, Tokyo, Japan). Regular detection for mycoplasma contamination was performed by Mycoplasma Detection Kit-QuickTest (Biotool, Houston, TX, USA).

Sotagliflozin treatment

For sotagliflozin treatment, cells were treated for 24 h with indicated doses of sotagliflozin dissolved in 10% dimethylsulfoxide (DMSO). After sotagliflozin treatment, medium was replaced with FBS-free DMEM, and cells were put under hypoxic condition as described above.

For HIF-1 α inhibition, cells were treated with 2-methoxyestradiol (2-ME2; Shanghai Macklin Biochemical, Shanghai, China; final concentration: 10 μ M) for 12 h, followed by sotagliflozin treatment as described above.

For *HIF-1 α* silencing experiment, C2C12 cells were transfected with control vector (shCon) or shRNA expression vector targeting *HIF-1 α* (shHIF-1 α) using Lipofectamine 2000 (Invitrogen Life Technologies, Grand Island, NY, USA) according to the manufacturer's instruction. Puromycin selection (2 μ g/mL) was performed 24 h after transfection for 48 h to eliminate untransfected cells.

Plasmids and constructs

For *HIF-1 α* silencing experiment, shRNA expression vectors targeting murine *HIF-1 α* (NM_001313919; target sites: 5'-GTGAAAGGATTCATATCTA-3' (shHIF-1 α -1), or 5'-GACACAGCCTC GATATGAA-3' (shHIF-1 α -2)) were constructed as described previously. Target sites were predicted as described previously [28]. For control vector (shCon), a vector containing a stretch of seven thymines downstream to the U6 promoter was used.

Animal experiment

Male C57BL/6 and Balb/c mice aged 6 weeks (body weight 15–20 g) were obtained from the Third Military Medical University (Chongqing, China). Animal studies were approved by the Laboratory Animal Welfare and Ethics Committee of the Third Military Medical University and performed in the Third Military Medical University. All animal studies conformed to the approved Guidelines for the Care and Use of Laboratory Animals of the Third Military Medical University. All efforts were made to minimize suffering.

For diabetes induction, C57BL/6 mice were fed with high fat diet for 3 weeks (20% kcal protein, 20% kcal carbohydrate, and 60% kcal fat). Intraperitoneal administration of 60 mg/kg body weight STZ diluted in sodium citrate buffer was then performed for the following 6 days. Mice were fasted overnight prior to each STZ injection and blood glucose level measurement. Blood glucose level was evaluated using Accu-Check Integra (Roche Diagnostics, Shanghai, China). Mice with blood glucose level ≥ 16.6 mM were assumed as diabetic mice, and were used for establishment of HLI model.

HLI model mice were established as described before [20]. Mice were anesthetized using pentobarbital sodium (100 mg/kg body weight). Surgery was performed by excising the femoral artery of the left hindlimb, while the corresponding right hindlimb was left without surgery and used as control. Mice were then grouped randomly. Starting from 24 h after surgery, sotagliflozin (10 mg/kg body weight) or equal volume of 10% DMSO was intramuscularly injected into the gastrocnemius muscle of the left hindlimb of the sotagliflozin-treated or control group, respectively, every 3 days for 21 days.

Damage caused by ischemia was evaluated with visual examination and scored as described previously (0 = no difference with control, 1 = mild change in color, 2 = moderate change in color, 3 = severe change in color, necrosis, loss of subcutaneous tissue, and 4 = lower-extremity amputation) at indicated time points [17, 29]. Blood perfusion in the hindlimb was visualized and analyzed by Laser Doppler Imager (Moor Instruments Ltd, Axminster, Devon, UK) at indicated time points. Prior to visualization, mice were anesthetized and the fur of the hindlimb area was depilated. Blood perfusion ratio was acquired by calculating the ratio between ischemic hindlimb (left) to corresponding control (right hindlimb) as described previously [17, 22, 30].

Conditioned media

Mature C2C12 cells were cultured in hyperglycemic condition as described above and treated with 10% DMSO or 10 μ M sotagliflozin for 24 h. Cells were then washed with PBS and exposed to hypoxia for 24 h. For control, cells were cultured in normoglycemic condition before being exposed to hypoxia for 24 h. Conditioned media collected from C2C12 cells cultured under normoglycemia and treated with 10% DMSO (CM-NG), as well as those collected from C2C12 cells cultured under hyperglycemia and treated with 10% DMSO or sotagliflozin (CM-HG or CM-HG + Sota, respectively) were obtained and filtered with 0.22 μ m filter (Sartorius, Germany) to eliminate cell debris.

Enzyme-linked immunosorbent assay (ELISA)

The amounts of VEGF-A and PDGF-BB in conditioned medium were determined using Mouse VEGF ELISA kit (Neobioscience, Shenzhen, China) and Mouse PDGF-BB ELISA kit (Neobioscience), respectively. ELISA was performed according to the manufacturer's guidelines.

EdU incorporation assay

Mature C2C12 cells were cultured under normoglycemic condition, or treated with 10 μ M sotagliflozin or an equal volume of 10% DMSO under hyperglycemia for 24 h, followed by exposure to hypoxia for 12 h as described above. EdU incorporation assay was performed using BeyoClick™ EdU-488 Cell Proliferation Assay Kit (Beyotime, Shanghai, China) according to the manufacturer's instruction. Images were obtained using Olympus IX73 (Olympus, Tokyo, Japan). Quantification was accomplished using ImageJ. Results were presented as the ratio of EdU-positive cells to those of Hoechst-positive cells. For experiments using the conditioned media, cells were cultured with CM-NG, CM-HG or CM-HG + Sota instead of DMEM prior to hypoxic treatment as described above.

Transwell migration assay

Mature C2C12 cells were cultured under normoglycemic condition, or treated with 10 μ M sotagliflozin or the same volume of 10% DMSO under hyperglycemic condition for 24 h. Cells were then re-seeded (5×10^3 per well) into the upper compartment of the transwell chamber and exposed to hypoxia for 24 h. Cells migrated to the lower compartment were stained using crystal violet (Beyotime). Visualization was achieved using Olympus IX71 (Olympus). For experiments using the conditioned media, HUVECs or MOVAS cells were seeded into the upper compartment, while the conditioned media were placed in the lower compartment of the transwell chambers prior to exposure to hypoxia.

Phalloidin staining

Mature C2C12 cells seeded in a glass bottom dish (4×10^3 per well) were cultured under normoglycemic condition, or treated with 10 μ M sotagliflozin or an equal volume of 10% DMSO under hyperglycemia for 24 h, and exposed to hypoxia 12 h. Prior to staining, cell fixation and permeabilization were employed by incubating the cells with 4% paraformaldehyde and 0.1% Triton X-100, respectively. Cells were then incubated with 1% bovine serum albumin, followed by phalloidin at room temperature for 60 min each. Images were obtained with Microsystems-TPS SP8 (Leica, Heidelberg, Germany). Fractal dimension analysis was accomplished using ImageJ. For experiments using conditioned media, HUVECs and MOVAS cells were cultured in the conditioned media for 24 h prior to being cultured under hypoxia for 12 h.

RNA extraction and quantitative reverse-transcription PCR (qRT-PCR)

Mature C2C12 cells were cultured under normoglycemic condition, or treated with indicated doses of sotagliflozin or an equal volume of 10% DMSO under hyperglycemia for 24 h. Cells were then serum-starved and exposed to hypoxia for 12 h, then total

RNA was extracted using Trizol (Invitrogen Life Technologies) according to manufacturer's instruction. Total RNA (1 μ g) was reverse-transcribed into cDNA using the PrimeScript RT Reagent Kit with gDNA Eraser (Takara Bio, Dalian, China). qRT-PCR was performed using SYBR Premix Ex Taq (Takara Bio). All primers used are listed in Supplementary Table S1. Data were shown as relative expression of mRNA level to the control, which was assumed as 1.

Western blotting analysis

Mature C2C12 cells were cultured in normoglycemic condition, or treated with indicated doses of sotagliflozin or an equal volume of 10% DMSO under hyperglycemia for 24 h. Cells were then exposed to hypoxia for 24 h prior to protein extraction using radioimmunoprecipitation assay (RIPA) lysis buffer with protease inhibitor and phosphatase inhibitor cocktail (complete cocktail, Roche Applied Science, Mannheim, Germany). For animal tissue, protein was extracted from the frozen gastrocnemius muscle of the ischemic limb using RIPA lysis buffer with protease inhibitor and phosphatase inhibitor cocktail (complete cocktail, Roche Applied Science, Mannheim, Germany). Detailed method for Western blotting was described previously [31]. Antibodies used are listed in Supplementary Table S2. β -Actin was used as loading control. Quantification was performed using Quantity One (Thermo Scientific, Waltham, MA, USA). Data were presented as relative to the control, which was assumed as 1.

Immunohistochemical staining

Gastrocnemius muscles were fixed in 4% paraformaldehyde before being embedded in paraffin. Tissues were then sliced at 4 μ m thickness using a cryostat, mounted on pre-coated glass slides, dewaxed using xylene, and then rehydrated. Antigen was retrieved by microwaving the sections in 10 mM sodium citrate buffer for 5 min followed by cooling for 20 min. Sections were treated with normal goat serum (Beyotime) for 1 h at room temperature to block nonspecific background staining, and incubated overnight at 4 °C with anti-HIF-1 α polyclonal antibody at a dilution of 1:200 (Zen-Bio, Chengdu, China). Endogenous peroxidase activity was blocked using 3% H₂O₂ in methanol for 3 min. Then the sections were incubated for 30 min with biotin-labeled goat anti-rabbit IgG serum (ZSGB-BIO, Beijing, China), followed by avidin-biotin-alkaline phosphatase complex (Vector Laboratories) for 30 min. After being washed with PBS, sections were developed in 3,3'-diaminobenzidine (DAB) chromogen solution, lightly counterstained with hematoxylin, dehydrated, and mounted. Images were obtained using Panoramic Midi (3DHitech, Budapest, Hungary). For hematoxylin and eosin (H&E) staining, sections were stained with Hematoxylin and Eosin (Beyotime) after being dewaxed and rehydrated as described above. Images were obtained using Olympus IX73 (Olympus).

Immunofluorescence staining

For immunofluorescence staining, gastrocnemius muscles from the ischemic hindlimb of HLI mice were sliced at 4 μ m thickness and stained for platelet-derived cell adhesion molecule-1 (PECAM-1) and alpha-smooth muscle actin (α -SMA) antibodies, as described previously [17]. Briefly, the tissue sections were incubated with PECAM-1 antibodies for 1 h, followed by incubation with monoclonal antibody against murine α -SMA conjugated with Cy3 and Alexa Fluor 488 Goat Anti-Rat IgG. Antibodies used in immunofluorescence staining are listed in Supplementary Table S2. Images were obtained with confocal microscopy (Leica, Microsystems-TPS SP8).

Cell viability and colony formation assay

Mature C2C12 cells were cultured in 96-well plates, treated with the indicated doses of sotagliflozin and cultured under hyperglycemic condition as described above. Cell proliferation assay was performed using MTS (Promega, Madison, WI, USA). Number of

viable cells was measured with a spectrophotometric microplate reader (BioTek Instruments, Winooski, VT, USA) at a wave length of 490 nm.

For colony formation assay, C2C12 cells were prepared as described above, re-seeded into six-well plates (50 cells per well) and grown for 14 days. Cells were fixed by 5 min incubation with 4% paraformaldehyde and stained using crystal violet (Beyotime). The numbers of colonies in each well were then counted.

Statistical analysis

Quantitative data were expressed as mean \pm SD ($n = 3$, unless further indicated). Statistical analysis of the blood perfusion ratio between time points in vivo was carried out using repeated-measures ANOVA, while difference between treatment groups was evaluated using one-way ANOVA. Morphological assessment was performed by a nonparametric Mann–Whitney test. Other statistical analysis was performed using Student's *t* test. Statistical analyses were performed using IBM SPSS Statistics v.17.0 (Armonk, NY, USA), and $P < 0.05$ was considered as statistically different.

RESULTS

Sotagliflozin enhances skeletal muscle cells' viability under hyperglycemia

Downregulation of skeletal muscle cells' viability by hyperglycemia leads to defective angiogenesis potential and poor prognosis; therefore, increasing their viability is critical for therapeutic

angiogenesis [32]. Hence, we first evaluated whether sotagliflozin could enhance skeletal muscle cells viability under hyperglycemia. To this end, we first induced the maturation of C2C12 cells by serum starvation as described previously [27], and confirmed their maturation by detecting the increase of myogenic differentiation (MyoD1) and myogenin (MyoG), two myogenic regulatory factors involved in the early and later stages of skeletal muscle differentiation, respectively (Supplementary Fig. S1). We next examined the effect of high glucose on cell viability, and confirmed that differentiated C2C12 cells viability was significantly decreased under hyperglycemia (Supplementary Fig. S2a, b). It is noteworthy that while glucose increased the osmotic pressure of the medium, culturing the differentiated C2C12 cells in 17.5 mM mannitol mimicking the osmotic pressure of the hyperglycemia did not significantly affect the cell viability compared to that of the normoglycemic medium, indicating that high glucose reduced cell viability irrespective of increased osmotic pressure [33, 34]. We then treated the differentiated C2C12 cells with different concentration of sotagliflozin under hyperglycemia. As shown in Fig. 1a, while hyperglycemia attenuated C2C12 cells viability, 48 h treatment with sotagliflozin could significantly increase it in a dose-dependent manner; however, there was only slight difference between treatment with 5, 10, or 20 μ M sotagliflozin. To determine the appropriate dose for further experiments, we prolonged the treatment to 72 h, and found that there was no significant difference between the effect of 10 and 20 μ M sotagliflozin on C2C12 cells viability (Fig. 1b). In line with this, sotagliflozin significantly enhanced

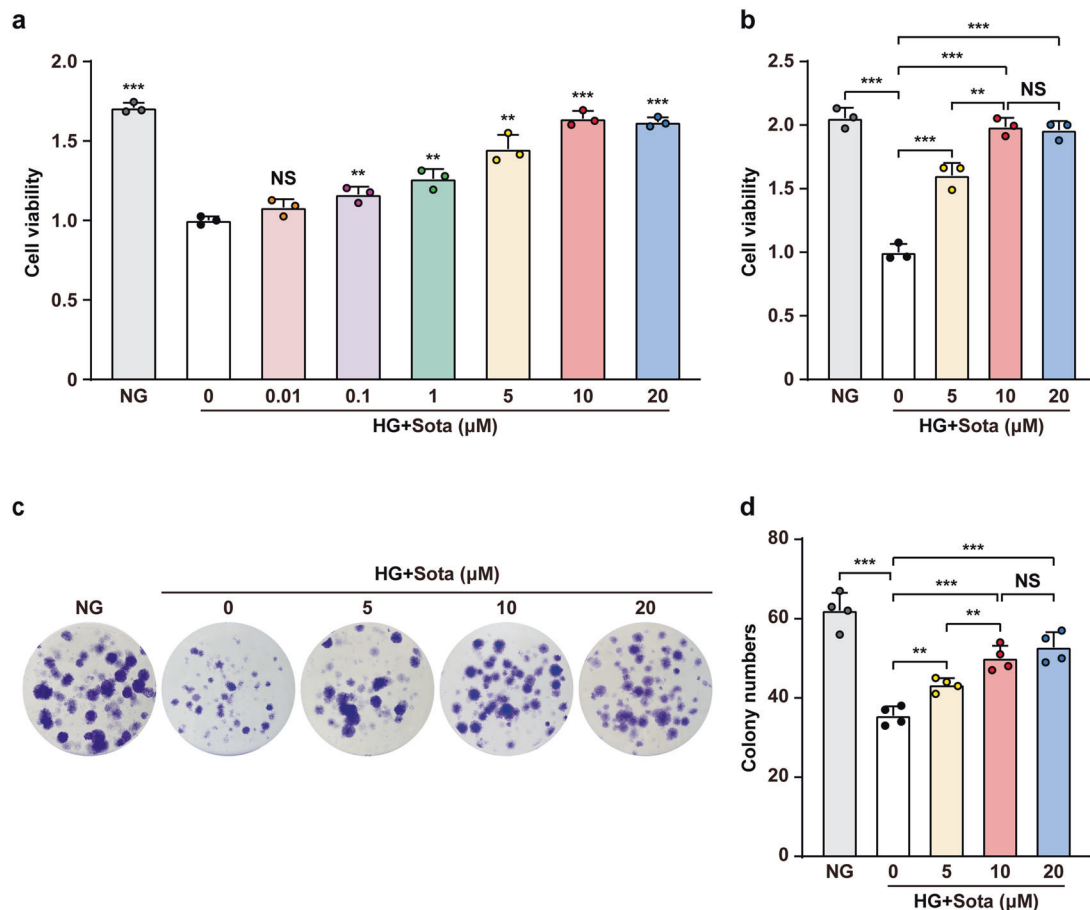


Fig. 1 Sotagliflozin improves cell viability in skeletal muscle cells under hyperglycemia. Total cell number of C2C12 cells treated with different doses of sotagliflozin and cultured under hyperglycemia for 48 h (a) or 72 h (b) ($n = 3$). c, d Effect of different dosages of sotagliflozin treatment on C2C12 cells viability as examined by colony formation assay. Representative images (c) and quantification results (d; $n = 4$) were shown. Cells cultured under normoglycemia were used as controls. Data were presented as mean \pm SD. NG normoglycemia, HG + Sota hyperglycemia + sotagliflozin, NS not significant; ** $P < 0.01$; *** $P < 0.001$.

colony numbers formed by C2C12 cells under hyperglycemia dose-dependently (Fig. 1c, d). Together, these results indicate that sotagliflozin could promote skeletal muscle cells viability. Furthermore, as both cell viability and colony formation assay showed that there was no significant difference between treatment with 10 μ M or higher concentration of sotagliflozin, we used 10 μ M sotagliflozin in further experiments.

Sotagliflozin promotes angiogenic factors expression in skeletal muscle cells

Skeletal muscle cells promote angiogenesis by expressing and secreting various angiogenic factors; however, hyperglycemia suppressed the expression levels of various angiogenic factors in matured C2C12 cells, while high osmotic did not result in significant effect (Supplementary Fig. S3a), indicating that high glucose concentration but not high osmotic pressure affected the potential of matured C2C12 cells in angiogenic factors expression. We then analyzed whether sotagliflozin could promote the expression levels of angiogenic factors in skeletal muscle cells under hyperglycemia. Sotagliflozin restored mRNA expression levels of VEGF-A, FGF2, PDGF-B, and HO-1 in C2C12 cells, which were suppressed under hyperglycemia (Fig. 2a). Examination of the accumulation of HIF-1 α protein, a transcription factor that regulates multiple angiogenic genes and is suppressed under hyperglycemia, demonstrated a significant restoration upon treatment with sotagliflozin (Fig. 2b, c). Similarly, the levels of VEGF-A, FGF2, PDGF-BB, and HO-1 protein were also restored. Furthermore, similar with the effect of sotagliflozin on skeletal muscle cells viability, the effect of sotagliflozin on abovementioned angiogenic factors also showed a dose-dependency (Fig. 2d, e). Moreover, sotagliflozin also promoted stromal cell-derived factor-1 (SDF-1)/CXCR4 chemokine receptor 4 (CXCR4) axis (Supplementary Fig. S3b), which is crucial for endothelial cells migration and adhesion [35]. As skeletal muscle cells cross-talk with blood vessels-forming cell is through their secretome, we next analyzed the amounts of VEGF-A and PDGF-BB in the medium. Sotagliflozin treatment clearly increased the levels of VEGF-A and PDGF-BB in the medium, indicating that it promoted the secretion levels of these factors (Fig. 2f). These results indicated that sotagliflozin could promote HIF-1 α protein accumulation and subsequently, angiogenic factors expression in skeletal muscle cells.

Sotagliflozin improves skeletal muscle cells proliferation and migration potentials

Skeletal muscle cells proliferation ability is important for providing sufficient angiogenic factors to form new blood vessels, while their migration ability is also crucial as it helps the dissemination of secreted angiogenic factors into larger ischemic areas [17]. To this end, we next analyzed the effect of sotagliflozin on proliferation and migration potentials of skeletal muscle cells under hyperglycemia. It is noteworthy that similar to the effects on cell viability and angiogenic factors expression levels, while hyperglycemia downregulated the ratio of EdU-positive C2C12 cells and the number of C2C12 cells migrated into the lower compartment of the transwell chamber, high osmotic pressure did not bring significant effect (Supplementary Fig. S4a, b). Meanwhile, sotagliflozin robustly increased the ratio of EdU-positive C2C12 cells, indicating the potential of sotagliflozin to enhance skeletal muscle cell proliferation (Fig. 3a, b). Furthermore, sotagliflozin increased the number of C2C12 cells migrated into the lower compartment of the transwell chamber, which was also suppressed by hyperglycemia, showing its stimulatory effect on skeletal muscle cells' migration potential (Fig. 3c, d). The effect of sotagliflozin on cell migration potential was further confirmed by phalloidin staining, revealing that sotagliflozin promoted F-Actin polymerization from G-Actin, an event that precede cell movements (Fig. 3e, f).

Sotagliflozin enhances skeletal muscle cells angiogenic potential under hyperglycemia in a HIF-1 α -dependent manner
HIF-1 α is a key regulator of multiple angiogenic factors, including VEGF-A and PDGF-BB, which are not only crucial for forming mature blood vessels [14, 17], but also could trigger autocrine signaling pathway to stimulate skeletal muscle cells' proliferation and migration potentials [36, 37]. To reveal the molecular mechanism underlying sotagliflozin regulation on skeletal muscle cells proliferation and migration potentials, we next examined whether HIF-1 α is involved in sotagliflozin regulation on skeletal muscle cells angiogenic potential. While sotagliflozin-induced HIF-1 α protein accumulation under hyperglycemia, treatment with 2-ME2, a HIF-1 α inhibitor [38], clearly abolished this effect. Furthermore, 2-ME2 suppressed sotagliflozin-enhanced VEGF-A and PDGF-BB protein levels in C2C12 cells under hyperglycemia (Fig. 4a, b). Similarly, 2-ME2 also suppressed the ratio of EdU-positive cells as well as the number of cells migrated to the lower chamber induced by sotagliflozin under hyperglycemia (Fig. 4c–f).

To further confirm the role of HIF-1 α in sotagliflozin regulation on C2C12 cells proliferation and migration potentials, we next silenced *HIF-1 α* in C2C12 cells using two shRNA expression vectors targeting different sites of *HIF-1 α* (Supplementary Fig. S5a–c). As the silencing effect of shHIF-1 α -2 was higher, we used it for further experiments. Indeed, *HIF-1 α* silencing abolished the effect of sotagliflozin in inducing VEGF-A and PDGF-BB mRNA (Fig. 5a) and protein (Fig. 5b, c) expression levels. Concomitantly, *HIF-1 α* silencing cancelled the increase of VEGF-A and PDGF-BB secretion induced by sotagliflozin (Fig. 5d, e). Furthermore, as presented in Fig. 5f–i, the stimulatory effects of sotagliflozin on skeletal muscle cells proliferation and migration potentials both decreased significantly in *HIF-1 α* -silenced C2C12 cells. Together, these results demonstrated that the pro-angiogenic effect of sotagliflozin on skeletal muscle cells occurs in a HIF-1 α -dependent manner.

Sotagliflozin increases the proliferation and migration potentials of vascular endothelial and smooth muscle cells via skeletal muscle cells secretome

Skeletal muscle cells contribute to angiogenesis by interacting with blood vessels-forming cells through their secretome [14]. To examine whether sotagliflozin could enhance the proliferation and migration potentials of blood vessels-forming cells through skeletal muscle cells secretome, we obtained conditioned media from C2C12 cells cultured under normoglycemia and treated with 10% DMSO (CM-NG), as well as from those cultured under hyperglycemia and treated with 10% DMSO or 10 μ M sotagliflozin (CM-HG and CM-HG + Sota, respectively). Compared to CM-NG, culturing vascular endothelial cells (HUVECs) using CM-HG significantly decreased the ratio of EdU-positive cells; however, CM-HG + Sota reversed this tendency (Fig. 6a, b). Similarly, CM-HG + Sota also restored the number of HUVECs cells migrated to the lower chamber of a transwell chamber, indicating that CM-HG + Sota restored endothelial cells migration potential which was disrupted when cultured with CM-HG (Fig. 6c, d), most plausibly due to the increase of F-Actin polymerization (Fig. 6e, f).

Similar to vascular endothelial cells, the ratio of EdU-positive smooth muscle cells (MOVAS cells) was suppressed when cultured with CM-HG, indicating that the angiogenic potential of secretome from skeletal muscle cells was disrupted when they were cultured under hyperglycemia (Fig. 7a, b). Meanwhile, the ratio of EdU-positive MOVAS cells was restored when cultured with CM-HG + Sota. Furthermore, CM-HG + Sota also restored the migration potential (Fig. 7c, d) as well as F-Actin polymerization (Fig. 7e, f) of MOVAS cells.

It is noteworthy that direct treatment of sotagliflozin did not enhance the expression levels of VEGF-A and PDGF-BB in HUVECs (Supplementary Fig. S6a, b), nor their proliferation and migration potentials (Supplementary Fig. S6c–f). Moreover, we also did not

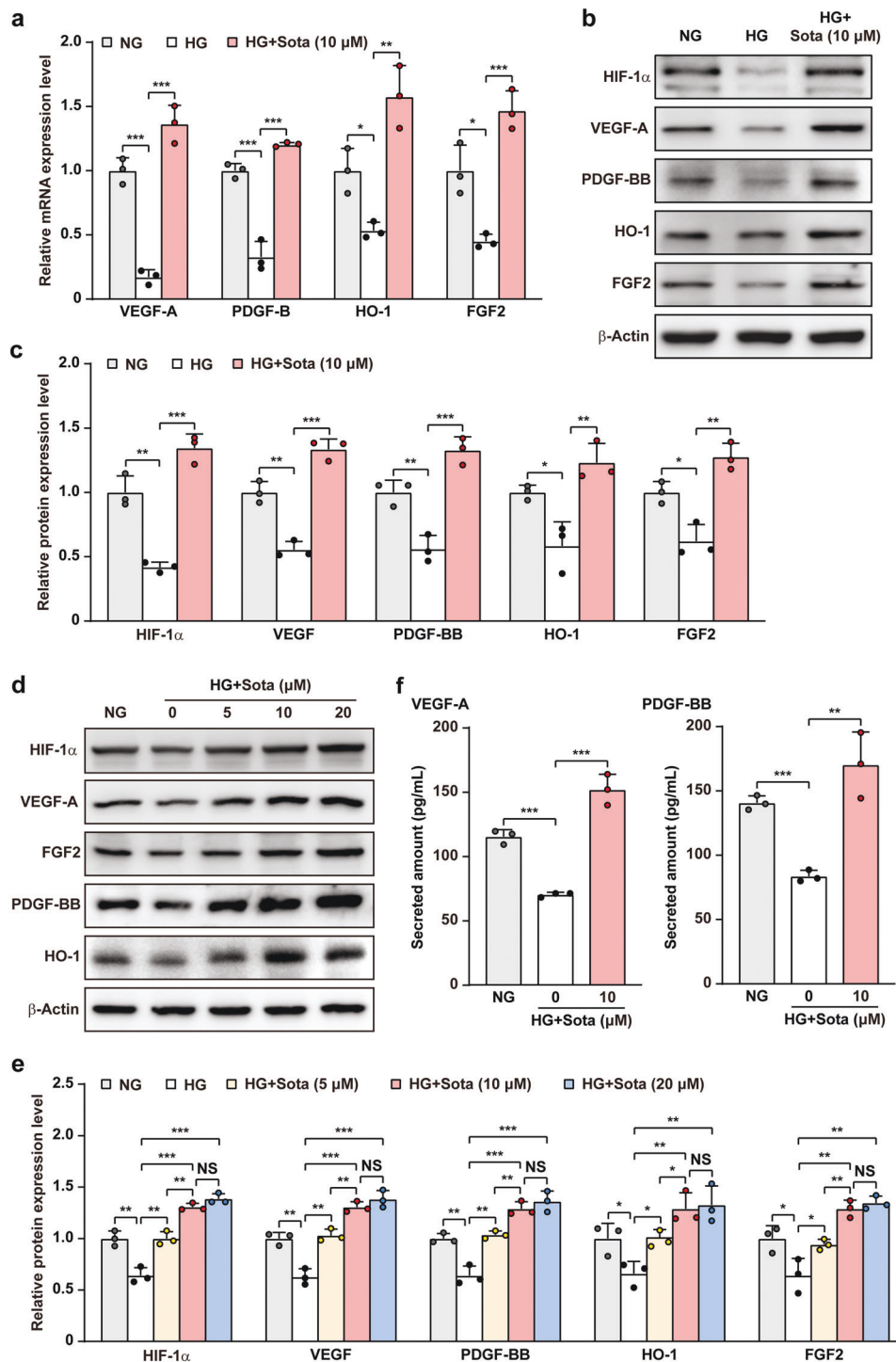


Fig. 2 Sotagliflozin promotes angiogenic factors expression in skeletal muscle cells under hyperglycemia. **a** mRNA expression levels of angiogenic factors in C2C12 cells treated with sotagliflozin under hyperglycemia, as examined using quantitative reverse-transcribed PCR (qRT-PCR). **b, c** Protein expression levels of angiogenic factors in C2C12 cells treated with sotagliflozin under hyperglycemia, as examined using Western blotting. Representative images (**b**) and quantification results (**c**) were shown. **d, e** Protein expression levels of angiogenic factors in C2C12 cells treated with different doses of sotagliflozin under hyperglycemia, as examined using Western blotting. Representative images (**d**) and quantification results (**e**) were shown. **f** Secreted amount of VEGF-A and PDGF-BB in the culture medium of matured C2C12 cells treated with sotagliflozin under hyperglycemia, as analyzed using ELISA. Cells cultured under normoglycemia were used as controls. β-Actin was used for qRT-PCR normalization and as Western blotting loading control. Quantitative data are shown as relative values to those of control, and expressed as mean ± SD ($n = 3$). NG normoglycemia, HG hyperglycemia, HG + Sota hyperglycemia + sotagliflozin, NS not significant; * $P < 0.05$; ** $P < 0.01$; *** $P < 0.001$.

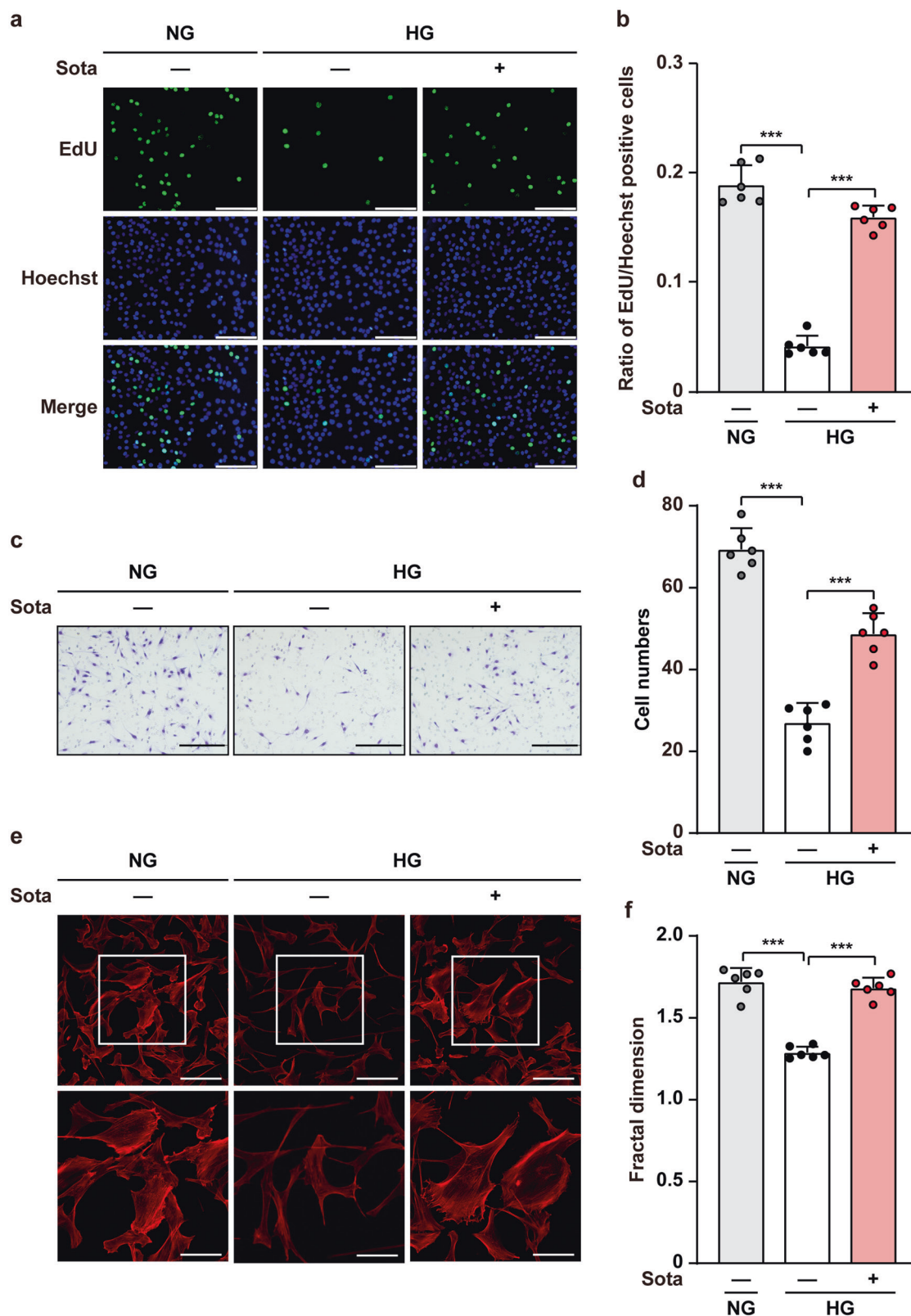


Fig. 3 Sotagliflozin enhances skeletal muscle cells proliferation and migration potentials under hyperglycemia. **a, b** Proliferation potential of C2C12 cells treated with 10 μ M sotagliflozin under hyperglycemia, as evaluated by EdU incorporation assay. Representative images (**a**; scale bars: 100 μ m) and quantification results (**b**) were shown. **c, d** Migration potential of C2C12 cells after 10 μ M sotagliflozin treatment, as investigated using transwell migration assay. Representative images (**c**; scale bars: 200 μ m) and quantification results (**d**) were shown. **e, f** F-Actin polymerization in C2C12 cells treated with 10 μ M sotagliflozin under hyperglycemia, as examined using phalloidin staining. Representative images (**e**; scale bars: 100 μ m for upper panels, 50 μ m for lower panels) and quantification of fractal dimension (**f**) were shown. Data were presented as mean \pm SD ($n = 6$). NG normoglycemia, HG hyperglycemia; *** $P < 0.001$.

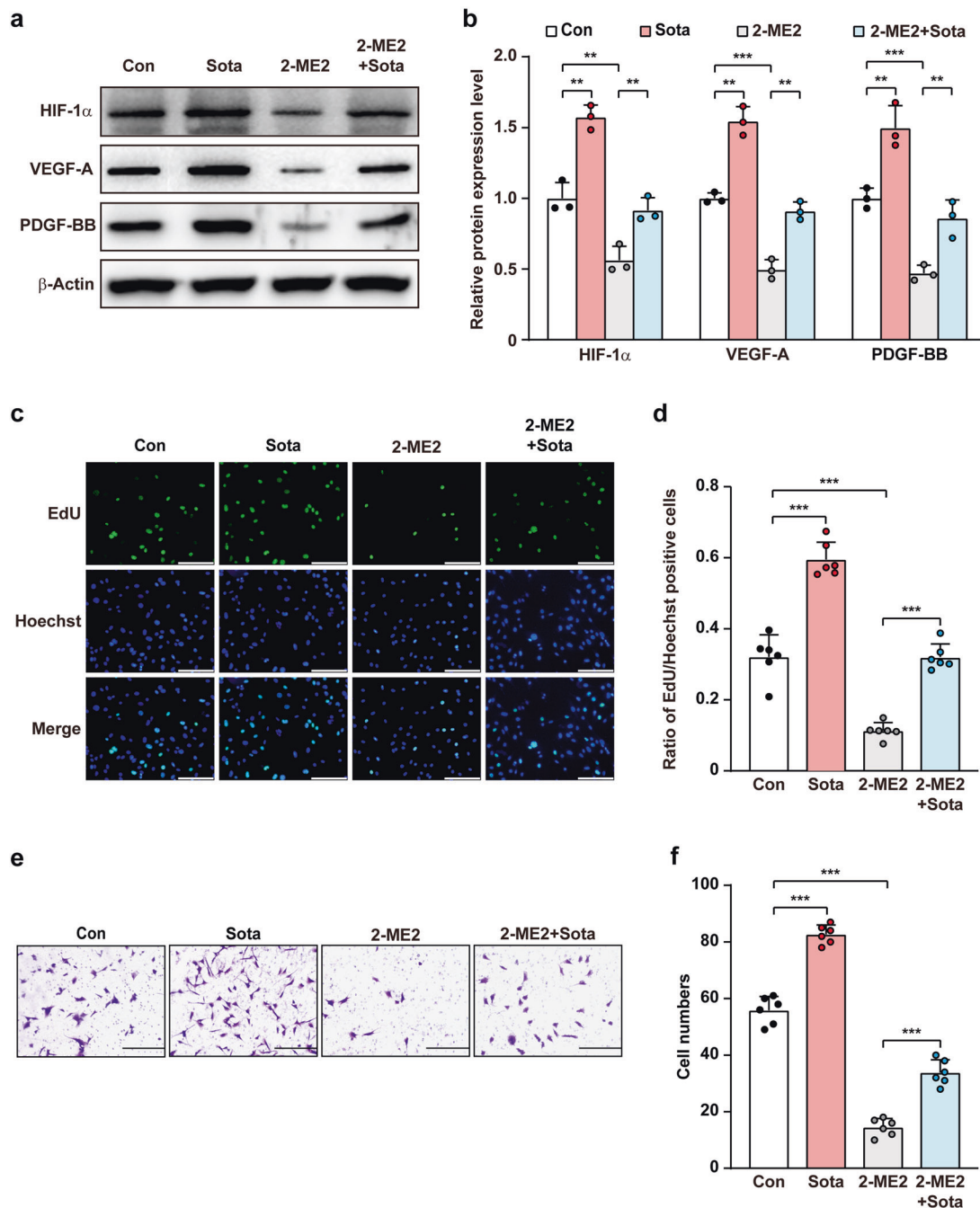


Fig. 4 Sotagliflozin enhances skeletal muscle cells angiogenesis potentials through HIF-1 α under hyperglycemia. **a, b** Protein expression levels of angiogenic factors in C2C12 cells treated with 10 μ M sotagliflozin and 2-ME2 under hyperglycemia, as examined using Western blotting. Representative images (**a**) and quantification results (**b**) were shown. **c, d** Proliferation potential of C2C12 cells treated with 10 μ M sotagliflozin and 2-ME2 under hyperglycemia, as evaluated by EdU incorporation assay. Representative images (**c**; scale bars: 100 μ m) and quantification results (**d**; $n = 6$) were shown. **e, f** Migration potential of C2C12 cells treated with 10 μ M sotagliflozin and 2-ME2 under hyperglycemia, as investigated using transwell migration assay. Representative images (**e**; scale bars: 200 μ m) and quantification results (**f**; $n = 6$) were shown. Cells treated with 10% DMSO under hyperglycemia were used as controls. β -Actin was used as Western blotting loading control. Data were presented as mean \pm SD ($n = 3$, unless further indicated). ** $P < 0.01$; *** $P < 0.001$.

observe any significant changes in the expression levels of VEGF-A and PDGF-BB, proliferation, and migration potentials of MOVAS cells treated directly with sotagliflozin (Supplementary Fig. S7a–f). Altogether, our results indicated that sotagliflozin could enhance the proliferation and migration potentials of blood vessels-forming cells by enhancing skeletal muscle cells' secretome-mediated cross-talk, but not through its direct effect on blood vessels-forming cells.

Sotagliflozin promotes neovascularization in diabetic HLI model mice
Finally, we examined whether sotagliflozin could promote neovascularization in diabetic and non-diabetic HLI mice. To this end, we established diabetic and non-diabetic HLI model mice by excising the left hindlimb femoral artery and administered sotagliflozin through intramuscular injection at the gastrocnemius muscle near the ischemic location, i.e., near the excision

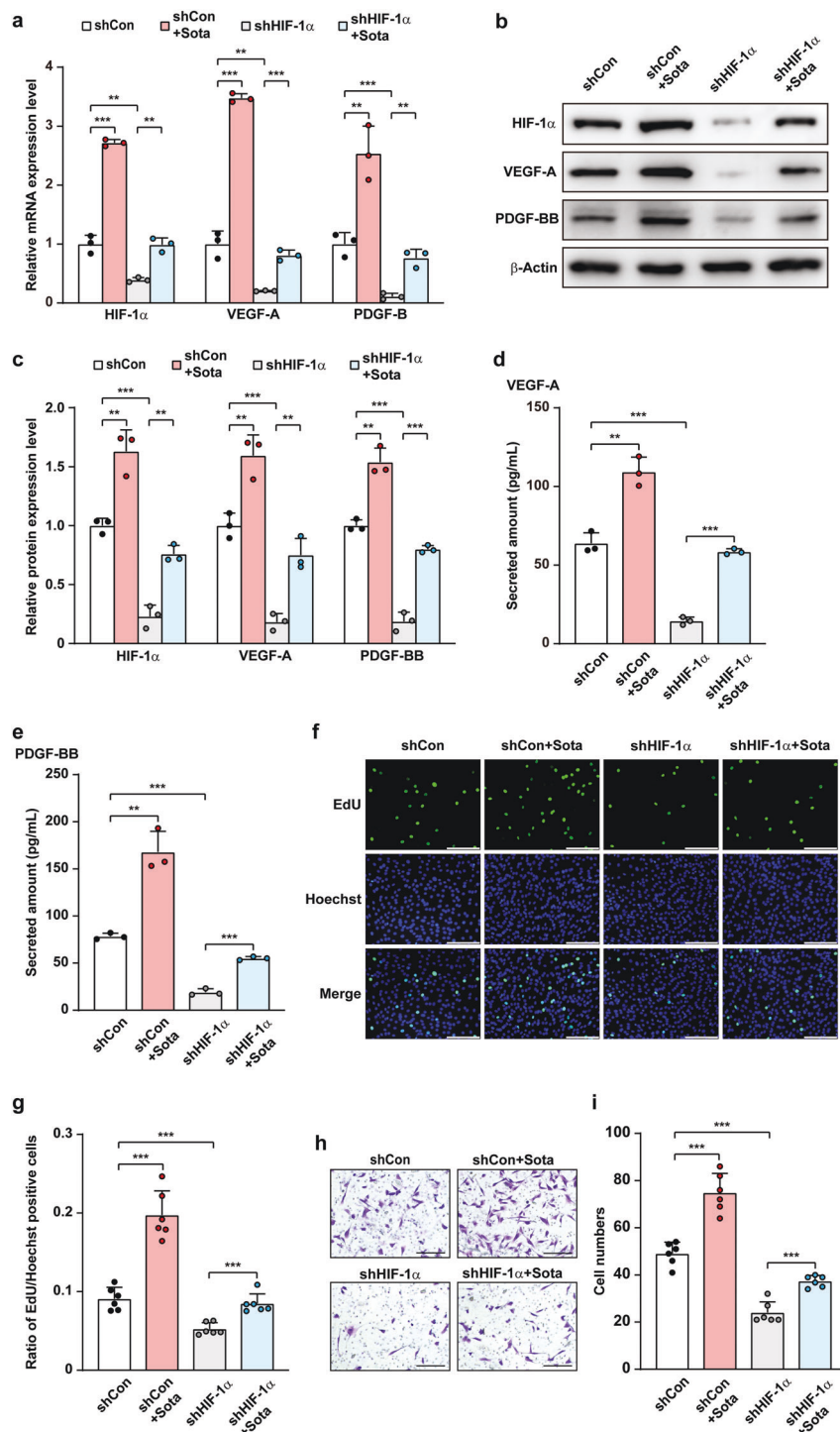


Fig. 5 Sotagliflozin promotes skeletal muscle cells angiogenesis potentials through HIF-1α under hyperglycemia. **a** mRNA expression levels of angiogenic factors in *HIF-1α*-knocked down C2C12 cells treated with 10 μM sotagliflozin under hyperglycemia, as examined using qRT-PCR. **b, c** Protein expression levels of angiogenic factors in *HIF-1α*-silenced C2C12 cells treated with 10 μM sotagliflozin under hyperglycemia, as examined using Western blotting. Representative images (**b**) and quantification results (**c**) were shown. Secreted amount of VEGF-A (**d**) and PDGF-BB (**e**) in the culture medium of *HIF-1α*-knocked down C2C12 cells treated with 10 μM sotagliflozin under hyperglycemia, as analyzed using ELISA. **f, g** Proliferation potential of *HIF-1α*-knocked down C2C12 cell treated with 10 μM sotagliflozin under hyperglycemia, as evaluated by EdU incorporation assay. Representative images (**f**; scale bars: 100 μm) and quantification results (**g**; $n = 6$) were shown. **h, i** Migration potential of *HIF-1α*-silenced C2C12 cells treated with 10 μM sotagliflozin under hyperglycemia, as investigated using transwell migration assay. Representative images (**h**; scale bars: 200 μm) and quantification results (**i**; $n = 6$) were shown. Cells transfected with shCon and treated with 10% DMSO under hyperglycemia were used as controls. β-Actin was used for qRT-PCR normalization and as Western blotting loading control. Data were presented as mean ± SD ($n = 3$, unless further indicated). ** $P < 0.01$; *** $P < 0.001$.

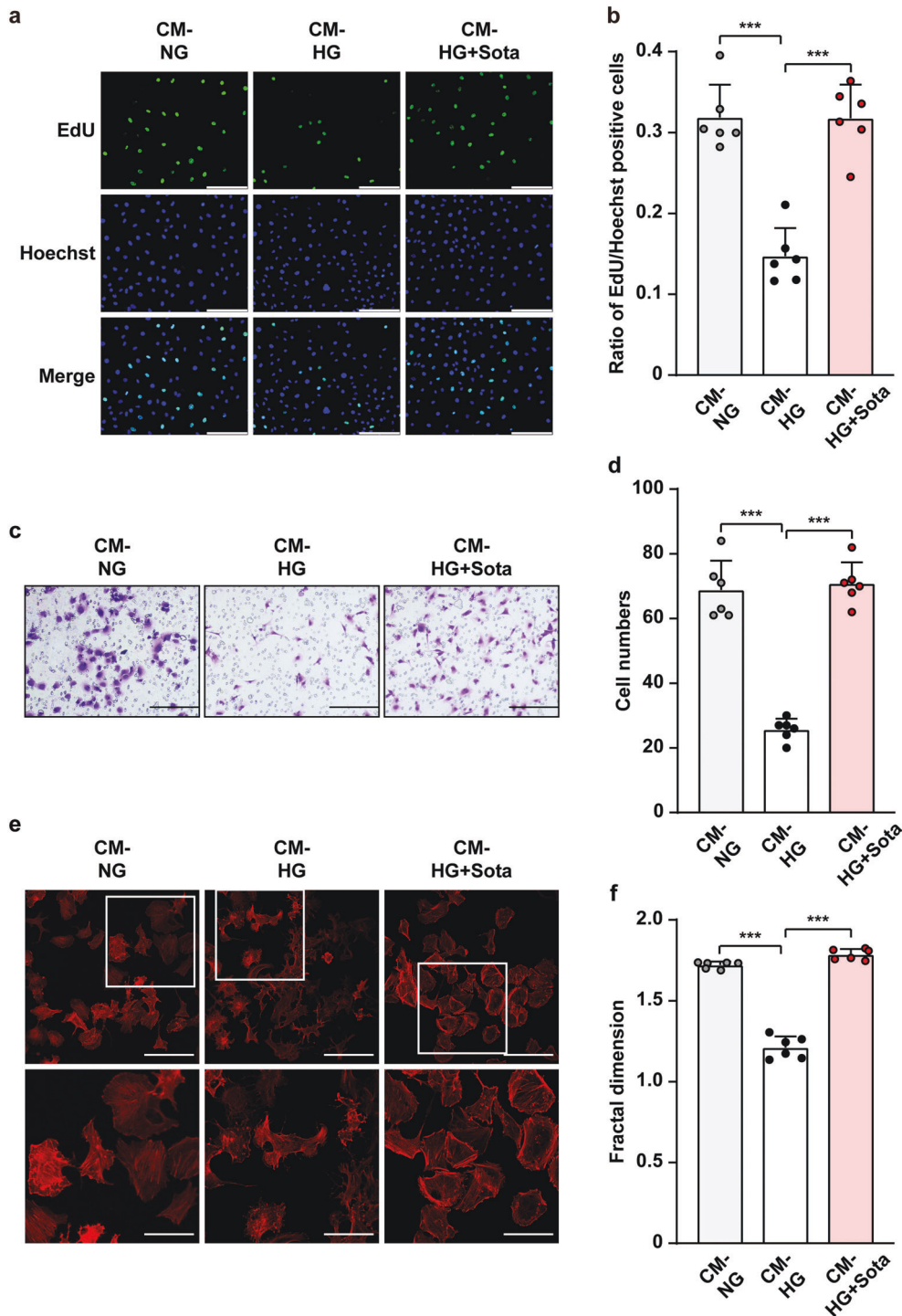


Fig. 6 Sotagliflozin enhances vascular endothelial cells migration and proliferation potentials under hyperglycemia through skeletal muscle cells' secretome. **a, b** Proliferation potential of HUVECs cultured with CM-HG + Sota, as examined using EdU incorporation assay. Representative images (**a**; scale bars: 100 μ m) and quantification results (**b**) were shown. **c, d** Migration potential of HUVECs cultured with CM-HG + Sota, as analyzed using transwell migration assay. Representative images (**c**; scale bars: 200 μ m) and quantification results (**d**) were shown. **e, f** F-Actin polymerization in HUVECs cultured with CM-HG + Sota, as examined using phalloidin staining. Representative images (**e**; scale bars: 100 μ m for upper panels and 50 μ m for lower panels) and quantification of fractal dimension (**f**) were shown. Data were presented as mean \pm SD ($n = 6$). CM-NG conditioned media obtained from 10% DMSO-treated C2C12 cells under normoglycemia, CM-HG conditioned media obtained from 10% DMSO-treated C2C12 cells under hyperglycemia, CM-HG + Sota conditioned media obtained from 10 μ M sotagliflozin-treated C2C12 cells under hyperglycemia; *** $P < 0.001$.

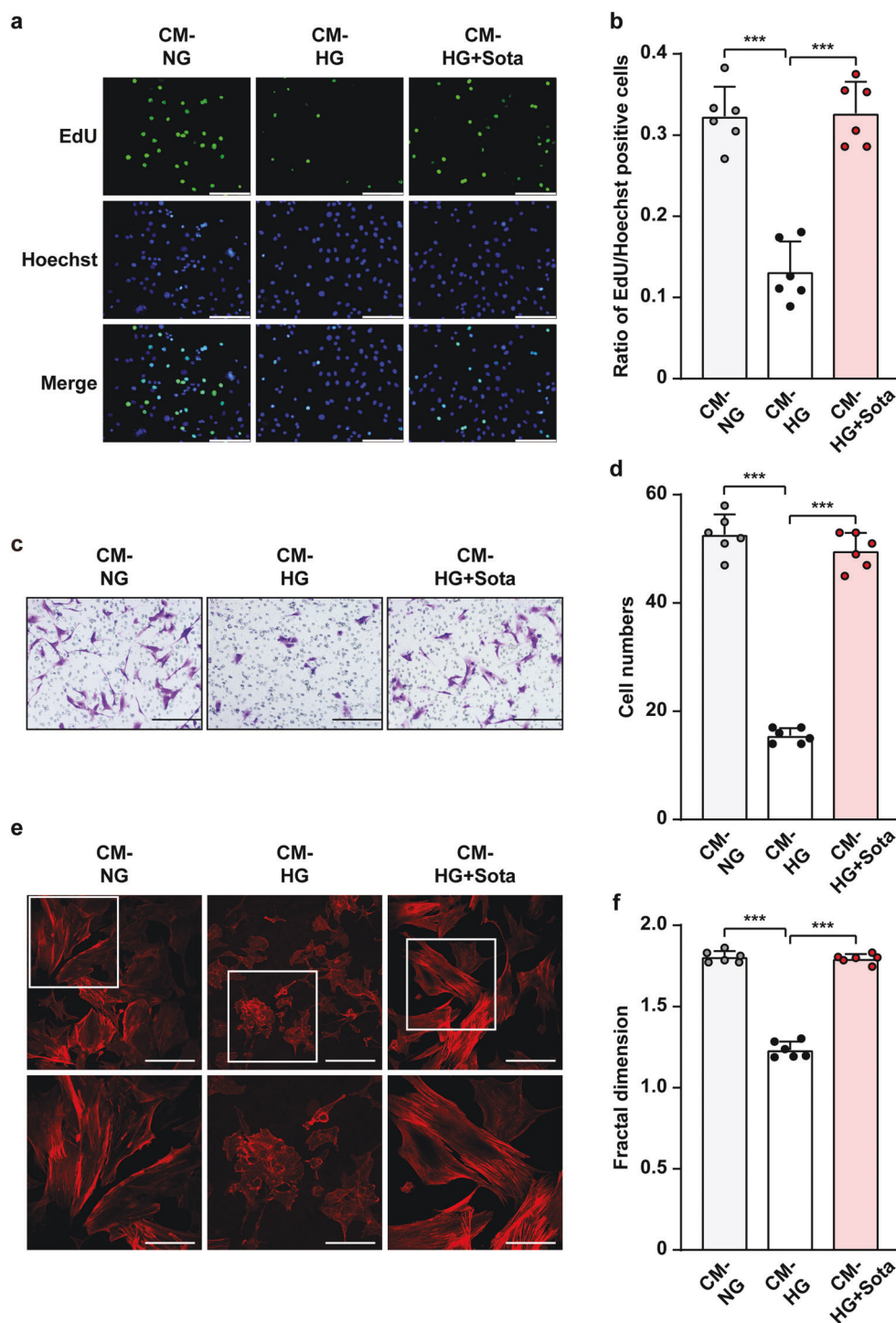


Fig. 7 Sotagliflozin enhances smooth muscle cells migration and proliferation potentials under hyperglycemia through skeletal muscle cells' secretome. **a, b** Proliferation potential of MOVAS cells, as examined using EdU incorporation assay. Representative images (**a**; scale bars; 100 μ m) and quantification results (**b**) were shown. **c, d** Migration potential of MOVAS cells cultured with CM-HG + Sota, as analyzed using transwell migration assay. Representative images (**c**; scale bars: 200 μ m) and quantification results (**d**) were shown. **e, f** F-Actin polymerization in MOVAS cells cultured with CM-HG + Sota, as examined using phalloidin staining. Representative images (**e**; scale bars: 100 μ m for upper panels and 50 μ m for lower panels) and quantifications of fractal dimension (**f**) were shown. Data were presented as mean \pm SD ($n = 6$). CM-NG conditioned media obtained from 10% DMSO-treated C2C12 cells under normoglycemia, CM-HG conditioned media obtained from 10% DMSO-treated C2C12 cells under hyperglycemia, CM-HG + Sota conditioned media obtained from 10 μ M sotagliflozin-treated C2C12 cells under hyperglycemia; *** $P < 0.001$.

location. Blood perfusion in both the left and the corresponding right hindlimb, which was used as control, was measured using Laser Doppler Imager. As shown in Fig. 8a, compared to that of control group which reached 30% blood perfusion recovery at day 21 after surgery, blood perfusion recovery in the ischemic hindlimb of diabetic HLI mice treated with sotagliflozin robustly increased starting from day 3 after surgery, and reached approximately 80% recovery at day 21 after surgery (Fig. 8a, b). Ischemic damage assessment further confirmed the positive effect of sotagliflozin (Fig. 8c), as sotagliflozin-treated diabetic HLI mice showed better limb morphologies, with most of the mice scoring 1, while most of the mice in the control group scored 3. Furthermore, although HLI in diabetic patients is harder to cure than in non-diabetic patients, HLI disease can also occur in non-diabetic patients [9, 39, 40], so we wondered if sotagliflozin would also be effective in inducing angiogenesis in non-diabetic HLI Balb/c mice. Indeed, intramuscular injection of sotagliflozin also significantly increased the recovery of blood perfusion in non-diabetic HLI Balb/c mice (Supplementary Fig. S8a, b). Together, these results clearly indicated the efficacy of sotagliflozin on enhancing blood perfusion recovery in both diabetic and non-diabetic HLI mice.

We then examined the potential mechanism behind the blood perfusion recovery induced by intramuscular injection of sotagliflozin. Immunofluorescence staining against PECAM-1, a marker of vascular endothelial cells, and α -SMA, a marker of smooth muscle cells, showed that sotagliflozin treatment noticeably increased the number of both PECAM-1- and α -SMA-positive cells (shown in green and red, respectively; Fig. 8d), as well as the number of PECAM-1-positive tube-like structures covered by α -SMA-positive cells (merged in yellow) in the ischemic hindlimb of diabetic HLI mice (Fig. 8d, e). Similarly, sotagliflozin treatment noticeably increased the number of both PECAM-1- and α -SMA-positive cells (Supplementary Fig. S8c), as well as the number of PECAM-1-positive tube-like structures covered by α -SMA-positive cells in the ischemic hindlimb of non-diabetic HLI mice (Supplementary Fig. S8d).

Next, we examined the expression level of HIF-1 α in the gastrocnemius muscle of diabetic HLI mice. As shown by immunohistochemical staining, sotagliflozin enhances the accumulation of HIF-1 α protein (Fig. 8f). This effect was further confirmed by Western blotting results (Fig. 8g, h). Furthermore, we confirmed robust increase of the protein expression levels of VEGF-A, FGF2, PDGF-BB, and HO-1 in the gastrocnemius muscle of the diabetic HLI mice treated with sotagliflozin. Taken together, our results suggested that intramuscular injection of sotagliflozin could enhance the formation of mature blood vessels in diabetic HLI mice. It is noteworthy that the blood glucose level of control group and sotagliflozin-treated group had no significant differences (Supplementary Table S3), indicating that the effect of sotagliflozin in improving blood perfusion in diabetic HLI mice was not due to the amelioration of hyperglycemic environment. Moreover, H&E staining of different organs in diabetic HLI mice showed that intramuscular injection of sotagliflozin had no significant effect on heart, liver, spleen, lung, kidney, and muscle tissues (Supplementary Fig. S9), as well as on mice's body weight (Supplementary Table S4), indicating that there was no significant toxicity of sotagliflozin administered intramuscularly.

Together, our results showed sotagliflozin promoted blood perfusion recovery by enhancing angiogenesis in diabetic HLI mice through its direct function on increasing HIF-1 α protein accumulation in skeletal muscle cells, thereby enhancing the expression of its downstream angiogenic factors. These factors in turn contribute to triggering the proliferation and migration capabilities of vascular endothelial and smooth muscle cells, thus effectively promoting angiogenesis by improving the formation of mature blood vessels in diabetic HLI model mice (Fig. 9).

DISCUSSION

Intrinsic angiogenesis potential is necessary for coupling with the damage in blood vessels; however, hyperglycemia adversely affects it [4]. Despite extensive and intensive researches, it is disappointing that vascular complications, mainly HLI [41], continue to compromise the quantity and quality of the lives of diabetic patients. While surgical-based direct revascularization strategy is not effective for diabetic HLI patients, therapeutic approach delivering angiogenic factors has become a promising strategy [13, 42]. Therapeutic angiogenesis aims to stimulate vessel formation and blood perfusion in order to alleviate hypoxic damages caused by insufficient oxygen supply into organs and tissues due to ischemia [43]. However, treatment with a single angiogenic factor could not produce effective neovascularization [44, 45], as it is a complex process of stimulating and promoting neovascularization, and forming new functional blood vessels requires a myriad of angiogenic factors and involves different type of cells.

Previous studies have reported that skeletal muscle is a prospective target for inducing effective and functional therapeutic angiogenesis, as it could secrete various angiogenic factors that lead to capillary growth [13, 17, 22]. However, due to impaired blood flow to the lower extremities, HLI reduced skeletal muscle capillary density and impaired muscle oxygen delivery [46]. This condition is even worse in diabetic patients, as hyperglycemia-induced systemic impairment could disrupt the paracrine and other cellular functions of skeletal muscle cells. Furthermore, recent studies uncovered that HIF-1 α , which plays a crucial role for coping with hypoxic stress, is destabilized under hyperglycemia, resulting in the loss of the cellular hypoxic responses including angiogenesis in most diabetic complications [19, 20]. Together, these lead to the aberrant decrease in angiogenic factors expression, subsequently deteriorating the endogenous angiogenesis potential in diabetic HLI patients [47]. Thus, the defect in endogenous angiogenesis potential is the obstacle for applying therapeutic angiogenesis strategy in diabetic HLI [48, 49], and stimulating this intrinsic potential is the key for successful therapeutic angiogenesis in diabetic HLI patients.

SGLT inhibitors, a new class of oral hypoglycemic agents, have been proven for its efficacy in reducing hyperglycemia [50]. In this study, we revealed that direct administration of SGLT inhibitor sotagliflozin into skeletal muscle cells increases their viability, proliferation, and migration potentials, as well as their paracrine function which are suppressed by hyperglycemia. This leads to the increase of VEGF-A, PDGF-BB, FGF2, and HO-1, as well as SDF-1/CXCR4 axis, which are crucial for mature and functional angiogenesis, and are targets of HIF-1 α [19–21, 51]. VEGF-A is an initiator of angiogenesis which induces the formation of the tube-like structure by endothelial cells; while FGF2 and PDGF-BB are crucial for vascular maturation. Meanwhile, HO-1 is a cell survival factor that suppresses oxidative stress-induced cellular damage and mitigates cellular injury [52]. SDF-1 is a member of the chemokine family that specifically binds to CXCR4 [53]. SDF-1/CXCR4 axis induces ischemic vessels to extend toward the areas with adequate blood supply by guiding endothelial cells migration and adhesion [35]. Collectively, our results show that although further investigation is required to examine if sotagliflozin also affects the levels of other angiogenic factors, its therapeutic effect on diabetic HLI mice could be attributed, at least partly, to the interplay between VEGF-A, FGF2, PDGF-BB, and HO-1. Our present findings give a new perspective for SGLT inhibitor sotagliflozin application as a potential clinical drug for diabetic HLI.

While our findings showed that intramuscularly-administrated sotagliflozin promotes angiogenesis in diabetic HLI, it is noteworthy that SGLT-2 inhibitors showed different effects on diabetic-associated vascular complications. Recent studies showed that while oral intake of empagliflozin and dapagliflozin, which lower cardiovascular morbidity and mortality in patients with type 2 diabetes, did not show increased risk of amputation [54, 55], oral

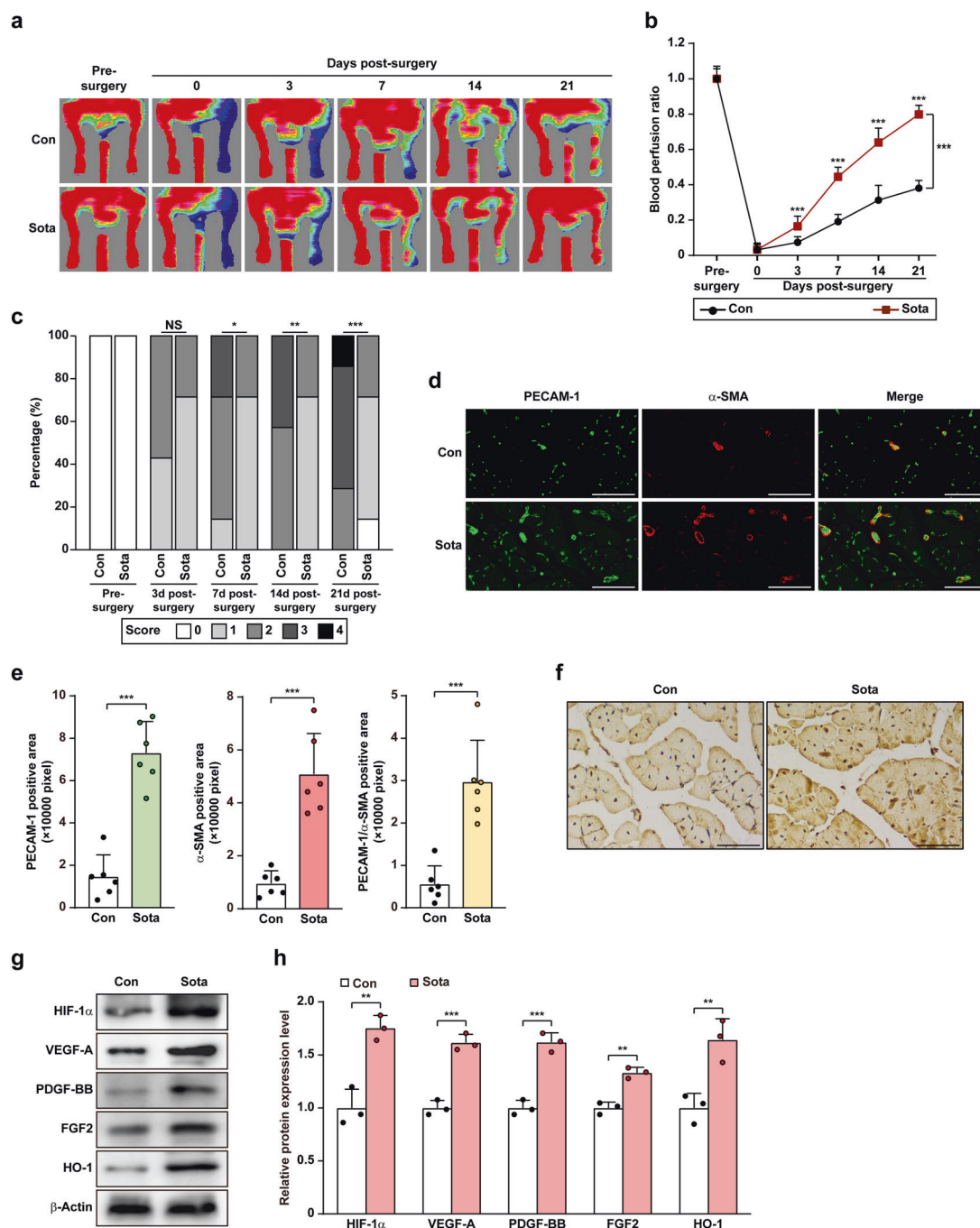


Fig. 8 Sotagliflozin enhances neovascularization in diabetic HLI mice. **a, b** Blood perfusion in the ischemic hindlimbs of diabetic HLI mice administered intramuscularly with sotagliflozin at indicated times. Representative images (**a**) and quantification data of blood perfusion ratio were shown (**b**; $n = 7$). **c** Morphological assessment of ischemic hindlimb in diabetic HLI mice intramuscularly injected with sotagliflozin at indicated time points ($n = 7$). **d, e** Immunofluorescence against PECAM-1 (green) and α -SMA (red) in ischemic hindlimbs tissue of diabetic HLI mice intramuscularly injected with sotagliflozin at day 21 after surgery. Representative images (**d**; scale bars: 50 μ m) and quantification results (**e**; $n = 6$) were shown. **f** Immunohistochemical staining of HIF-1 α in ischemic hindlimbs tissue of diabetic HLI mice intramuscularly injected with sotagliflozin at day 21 after surgery. Representative images (scale bars: 50 μ m) were shown. **g, h** Protein expression levels of angiogenic factors in the ischemic hindlimbs of diabetic HLI mice intramuscularly injected with sotagliflozin, as examined using Western blotting. Representative images (**g**) and quantification results (**h**) were shown. β -Actin was used as Western blotting loading control. Quantitative data were presented as mean \pm SD ($n = 3$, unless further indicated). Con mice were administered with 10% DMSO, Sota mice were administered with sotagliflozin (10 mg/kg body weight), NS not significant; * $P < 0.05$; ** $P < 0.01$; *** $P < 0.001$.

administration of canagliflozin inhibits tube formation, thus increasing the risk of limb amputation [56, 57]. Meanwhile, although sotagliflozin is known as an oral anti-hyperglycemic drug, we found that its intramuscular injection did not cause significant change in blood glucose levels of diabetic HLI mice.

These distinct effects are most plausibly due to the difference in administration method, as orally-administered sotagliflozin might be metabolized and distributed systemically, while intramuscular injection provided a more localized and direct effect of sotagliflozin. Furthermore, direct sotagliflozin treatment could not

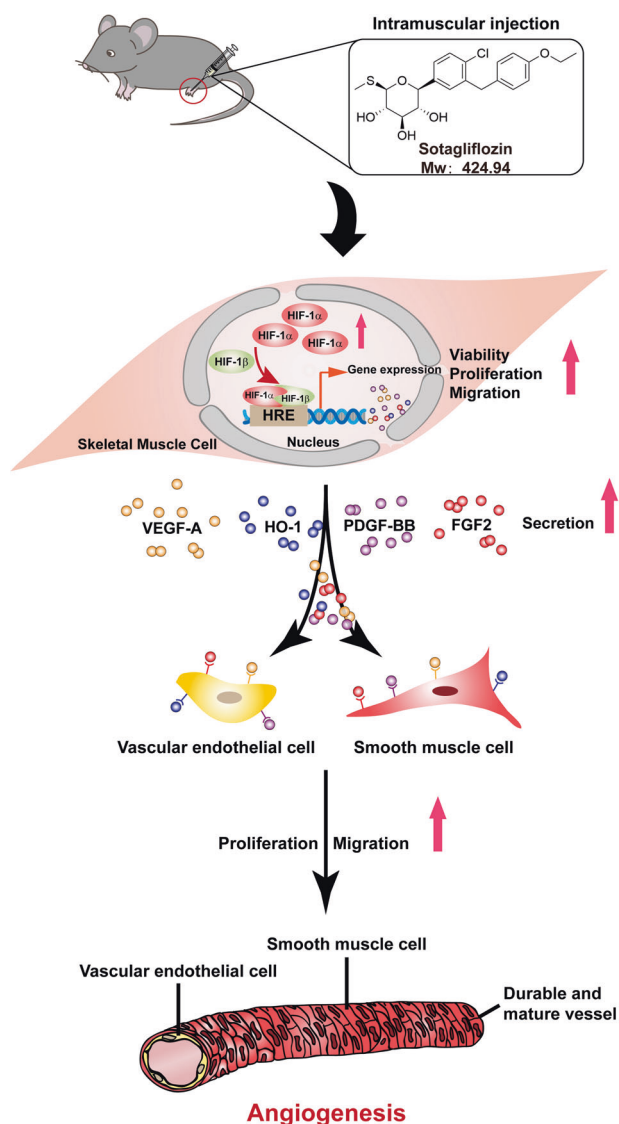


Fig. 9 Schematic diagram of the effect of SGLT2 inhibitor sotagliflozin on facilitating therapeutic angiogenesis in diabetic HLI mice. Sotagliflozin promotes the viability, proliferation, and migration potentials of skeletal muscle cells, and enhances the expression of angiogenic factors in skeletal muscle cells of diabetic HLI mice. These angiogenic factors in turn trigger proliferation and migration potentials of blood-vessels forming cells, and subsequently promotes therapeutic angiogenesis in diabetic HLI model mice.

affect the viability, proliferation and migration potentials of vascular endothelial and smooth muscle cells, indicating that these direct effects of sotagliflozin might be cell-type specific. Therefore, while further intensive studies are needed to elucidate the detailed molecular mechanism, these facts indicate that different SGLT2 inhibitors might have distinct functions dependent on the compound structure, the administration method, as well as on the target cell types.

In conclusion, our results described a novel function of SGLT2 inhibitor sotagliflozin in protecting skeletal muscle cells and promoting angiogenesis under hyperglycemia. Sotagliflozin restores HIF-1α protein accumulation in skeletal muscle cells disrupted by hyperglycemia, leading to the restoration of their angiogenic potential, which, as a consequence, promotes the proliferation and migration capabilities of vascular endothelial and

smooth muscle cells. These in turn promoted the formation of mature and functional blood vessels and, subsequently, improved the recovery of blood perfusion in diabetic HLI mice. While further pre-clinical and clinical studies are necessary, this study highlighted the potential application of sotagliflozin as a small molecule drug for therapeutic angiogenesis strategy for treating diabetic and non-diabetic HLI.

ACKNOWLEDGEMENTS

This work was supported by grants from the National Natural Science Foundation of China (31871367 and 81872273), and the Natural Science Foundation of Chongqing (cstc2018jcyjAX0411).

AUTHOR CONTRIBUTIONS

VK and SRW arranged the research, designed the experiments, examined and construed the data, wrote the manuscript, provided financial support, and guided all the experiments. LLL and JXH performed the cellular and animal experiments, examined and construed the data, and wrote the manuscript.

ADDITIONAL INFORMATION

Supplementary information The online version contains supplementary material available at <https://doi.org/10.1038/s41401-022-00889-4>.

Competing interests: The authors declare no competing interests. A Chinese patent related to the results of this study has been filed with patent application No. 202010701077.7.

REFERENCES

- Edgerton DS, Kraft G, Smith M, Farmer B, Williams PE, Coate KC, et al. Insulin's direct hepatic effect explains the inhibition of glucose production caused by insulin secretion. *JCI Insight*. 2017;2:e91863.
- Zheng Y, Ley SH, Hu FB. Global aetiology and epidemiology of type 2 diabetes mellitus and its complications. *Nat Rev Endocrinol*. 2018;14:88–98.
- McGuire S. World cancer report 2014. Geneva, Switzerland: World health organization, international agency for research on cancer, WHO press, 2015. *Adv Nutr*. 2016;7:418–9.
- American Diabetes A. Diagnosis and classification of diabetes mellitus. *Diabetes Care*. 2010;33:S62–9.
- Bluestone JA, Buckner JH, Herold KC. Immunotherapy: building a bridge to a cure for type 1 diabetes. *Science*. 2021;373:510–6.
- Buchwald H, Buchwald JN. Metabolic (bariatric and nonbariatric) surgery for type 2 diabetes: a personal perspective review. *Diabetes Care*. 2019;42:331–40.
- Costa PZ, Soares R. Neovascularization in diabetes and its complications. Unraveling the angiogenic paradox. *Life Sci*. 2013;92:1037–45.
- Criqui MH, Matsushita K, Aboyans V, Hess CN, Hicks CW, Kwan TW, et al. Lower extremity peripheral artery disease: Contemporary epidemiology, management gaps, and future directions: a scientific statement from the American heart association. *Circulation*. 2021;144:e171–e91.
- Jude EB, Oyibo SO, Chalmers N, Boulton AJ. Peripheral arterial disease in diabetic and nondiabetic patients: A comparison of severity and outcome. *Diabetes Care*. 2001;24:1433–7.
- Gerhard-Herman MD, Gornik HL, Barrett C, Barshes NR, Corriere MA, Drachman DE, et al. AHA/ACC guideline on the management of patients with lower extremity peripheral artery disease: Executive summary: A report of the American college of cardiology/American heart association task force on clinical practice guidelines. *Circulation*. 2017;135:e686–e725.
- Norgren L, Hiatt WR, Dormandy JA, Nehler MR, Harris KA, Fowkes FG, et al. Inter-society consensus for the management of peripheral arterial disease (TASC II). *Eur J Vasc Endovasc Surg*. 2007;33:S1–75.
- Demir S, Nawroth PP, Herzig S, Ekim Ustunel B. Emerging targets in type 2 diabetes and diabetic complications. *Adv Sci*. 2021;8:e2100275.
- Tateno K, Minamino T, Toko H, Akazawa H, Shimizu N, Takeda S, et al. Critical roles of muscle-secreted angiogenic factors in therapeutic neovascularization. *Circ Res*. 2006;98:1194–202.
- Giudice J, Taylor JM. Muscle as a paracrine and endocrine organ. *Curr Opin Pharmacol*. 2017;34:49–55.
- Ariyanti AD, Sisjayawan J, Zhang J, Zhang JQ, Wang GX, Miyagishi M, et al. Elevating VEGF-A and PDGF-BB secretion by salidroside enhances neovascularization in diabetic hind-limb ischemia. *Oncotarget*. 2017;8:97187–205.

16. Karsenty G, Olson EN. Bone and muscle endocrine functions: Unexpected paradigms of inter-organ communication. *Cell*. 2016;164:1248–56.
17. Zhang J, Kasim V, Xie YD, Huang C, Sisjayawan J, Dwi Ariyanti A, et al. Inhibition of PHD3 by salidroside promotes neovascularization through cell-cell communications mediated by muscle-secreted angiogenic factors. *Sci Rep*. 2017;7:43935.
18. Majesky MW. Vascular development. *Arterioscler Thromb Vasc Biol*. 2018;38:e17–e24.
19. Botusan IR, Sunkari VG, Savu O, Catrina AI, Grunler J, Lindberg S, et al. Stabilization of HIF-1alpha is critical to improve wound healing in diabetic mice. *Proc Natl Acad Sci USA*. 2008;105:19426–31.
20. Wu S, Nishiyama N, Kano MR, Morishita Y, Miyazono K, Itaka K, et al. Enhancement of angiogenesis through stabilization of hypoxia-inducible factor-1 by silencing prolyl hydroxylase domain-2 gene. *Mol Ther*. 2008;16:1227–34.
21. Semenza GL. Regulation of vascularization by hypoxia-inducible factor 1. *Ann NY Acad Sci*. 2009;1177:2–8.
22. Wu S, Zhang J, Huang C, Jia H, Wang Y, Xu Z, et al. Prolyl hydroxylase domain-2 silencing induced by hydrodynamic limb vein injection enhances vascular regeneration in critical limb ischemia mice through activation of multiple genes. *Curr Gene Ther*. 2015;15:313–25.
23. Zhang J, Nugrahaningrum DA, Marcelina O, Ariyanti AD, Wang G, Liu C, et al. Tyrosol facilitates neovascularization by enhancing skeletal muscle cells viability and paracrine function in diabetic hindlimb ischemia mice. *Front Pharmacol*. 2019;10:909.
24. Cefalo CMA, Cinti F, Moffa S, Impronta F, Sorice GP, Mezza T, et al. Sotagliflozin, the first dual sglT inhibitor: Current outlook and perspectives. *Cardiovasc Diabetol*. 2019;18:20.
25. Bhatt DL, Szarek N, Steg PG, Cannon CP, Leiter LA, McGuire DK, et al. Sotagliflozin in patients with diabetes and recent worsening heart failure. *N Engl J Med*. 2021;384:117–28.
26. Bhatt DL, Szarek M, Pitt B, Cannon CP, Leiter LA, McGuire DK, et al. Sotagliflozin in patients with diabetes and chronic kidney disease. *N Engl J Med*. 2021;384:129–39.
27. Lawson MA, Purslow PP. Differentiation of myoblasts in serum-free media: effects of modified media are cell line-specific. *Cells Tissues Organs*. 2000;167:130–7.
28. Miyagishi M, Taira K. Strategies for generation of an sirna expression library directed against the human genome. *Oligonucleotides*. 2003;13:325–33.
29. Stabile E, Burnett MS, Watkins C, Kinnaird T, Bachis A, la Sala A, et al. Impaired arteriogenic response to acute hindlimb ischemia in CD4-knockout mice. *Circulation*. 2003;108:205–10.
30. Tani M, Yonemitsu Y, Fujii T, Shikada Y, Kohno R, Onimaru M, et al. Diabetic microangiopathy in ischemic limb is a disease of disturbance of the platelet-derived growth factor-BB/protein kinase C axis but not of impaired expression of angiogenic factors. *Circ Res*. 2006;98:55–62.
31. Wu S, Wang H, Li Y, Xie Y, Huang C, Zhao H, et al. Transcription factor YY1 promotes cell proliferation by directly activating the pentose phosphate pathway. *Cancer Res*. 2018;78:4549–62.
32. Ariyanti AD, Zhang J, Marcelina O, Nugrahaningrum DA, Wang G, Kasim V, et al. Salidroside-pretreated mesenchymal stem cells enhance diabetic wound healing by promoting paracrine function and survival of mesenchymal stem cells under hyperglycemia. *Stem Cells Transl Med*. 2019;8:404–14.
33. Chen YH, Lin SJ, Lin FY, Wu TC, Tsao CR, Huang PH, et al. High glucose impairs early and late endothelial progenitor cells by modifying nitric oxide-related but not oxidative stress-mediated mechanisms. *Diabetes*. 2007;56:1559–68.
34. Racz B, Reglodi D, Fodor B, Gasz B, Lubics A, Gallyas F Jr, et al. Hyperosmotic stress-induced apoptotic signaling pathways in chondrocytes. *Bone*. 2007;40:1536–43.
35. Young KC, Torres E, Hatzistergos KE, Hehre D, Suguihara C, Hare JM. Inhibition of the SDF-1/CXCR4 axis attenuates neonatal hypoxia-induced pulmonary hypertension. *Circ Res*. 2009;104:1293–301.
36. Germani A, Di Carlo A, Mangoni A, Straino S, Giacinti C, Turrini P, et al. Vascular endothelial growth factor modulates skeletal myoblast function. *Am J Pathol*. 2003;163:1417–28.
37. Wang CG, Lou YT, Tong MJ, Zhang LL, Zhang ZJ, Feng YZ, et al. Asperosaponin VI promotes angiogenesis and accelerates wound healing in rats via up-regulating HIF-1alpha/VEGF signaling. *Acta Pharmacol Sin*. 2018;39:393–404.
38. Masoud GN, Li W. Hif-1alpha pathway: Role, regulation and intervention for cancer therapy. *Acta Pharm Sin B*. 2015;5:378–89.
39. Chen X, Duong MN, Psaltis PJ, Bursill CA, Nicholls SJ. High-density lipoproteins attenuate high glucose-impaired endothelial cell signaling and functions: Potential implications for improved vascular repair in diabetes. *Cardiovasc Diabetol*. 2017;16:121.
40. Baumgartner-Parzer SM, Wagner L, Pettermann M, Grillari J, Gessl A, Waldhausl W. High-glucose-triggered apoptosis in cultured endothelial cells. *Diabetes*. 1995;44:1323–7.
41. Hazarika S, Dokun AO, Li Y, Popel AS, Kontos CD, Annex BH. Impaired angiogenesis after hindlimb ischemia in type 2 diabetes mellitus: differential regulation of vascular endothelial growth factor receptor 1 and soluble vascular endothelial growth factor receptor 1. *Circ Res*. 2007;101:948–56.
42. Forster R, Liew A, Bhattacharya V, Shaw J, Stansby G. Gene therapy for peripheral arterial disease. *Cochrane Database Syst Rev*. 2018;10:CD012058.
43. Annex BH. Therapeutic angiogenesis for critical limb ischaemia. *Nat Rev Cardiol*. 2013;10:387–96.
44. Celletti FL, Waugh JM, Amabile PG, Brendolan A, Hilfiker PR, Dake MD. Vascular endothelial growth factor enhances atherosclerotic plaque progression. *Nat Med*. 2001;7:425–9.
45. Epstein AC, Gleadle JM, McNeill LA, Hewitson KS, O'Rourke J, Mole DR, et al. C. Elegans EGL-9 and mammalian homologs define a family of dioxygenases that regulate HIF by prolyl hydroxylation. *Cell*. 2001;107:43–54.
46. McDermott MM, Ferrucci L, Gonzalez-Freire M, Kosmac K, Leeuwenburgh C, Peterson CA, et al. Skeletal muscle pathology in peripheral artery disease: a brief review. *Arterioscler Thromb Vasc Biol*. 2020;40:2577–85.
47. Perez-Ilzarbe M, Agbulut O, Pelacho B, Ciorba C, San Jose-Eneriz E, Desnos M, et al. Characterization of the paracrine effects of human skeletal myoblasts transplanted in infarcted myocardium. *Eur J Heart Fail*. 2008;10:1065–72.
48. Jude EB, Eleftheriadou I, Tentolouris N. Peripheral arterial disease in diabetes—a review. *Diabet Med*. 2010;27:4–14.
49. Rask-Madsen C, King GL. Vascular complications of diabetes: mechanisms of injury and protective factors. *Cell Metab*. 2013;17:20–33.
50. Chao EC, Henry RR. SGLT2 inhibition—a novel strategy for diabetes treatment. *Nat Rev Drug Discov*. 2010;9:551–9.
51. Youn SW, Lee SW, Lee J, Jeong HK, Suh JW, Yoon CH, et al. COMP-Ang1 stimulates HIF-1alpha-mediated SDF-1 overexpression and recovers ischemic injury through BM-derived progenitor cell recruitment. *Blood*. 2011;117:4376–86.
52. Gou L, Zhao L, Song W, Wang L, Liu J, Zhang H, et al. Inhibition of miR-92a suppresses oxidative stress and improves endothelial function by upregulating heme oxygenase-1 in *db/db* mice. *Antioxid Redox Signal*. 2018;28:358–70.
53. Li M, Hale JS, Rich JN, Ransohoff RM, Lathia JD. Chemokine CXCL12 in neurodegenerative diseases: an SOS signal for stem cell-based repair. *Trends Neurosci*. 2012;35:619–28.
54. Heyward J, Mansour O, Olson L, Singh S, Alexander GC. Association between sodium-glucose cotransporter 2 (SGLT2) inhibitors and lower extremity amputation: a systematic review and meta-analysis. *PLoS One*. 2020;15:e0234065.
55. Sung J, Padmanabhan S, Gurung S, Inglis S, Vicaretti M, Begg L, et al. SGLT2 inhibitors and amputation risk: real-world data from a diabetes foot wound clinic. *J Clin Transl Endocrinol*. 2018;13:46–47.
56. Matthews DR, Li Q, Perkovic V, Mahaffey KW, de Zeeuw D, Fulcher G, et al. Effects of canagliflozin on amputation risk in type 2 diabetes: The CANVAS program. *Diabetologia*. 2019;62:926–38.
57. Birkeland KI, Jorgensen ME, Carstensen B, Persson F, Gulseth HL, Thuesen M, et al. Cardiovascular mortality and morbidity in patients with type 2 diabetes following initiation of sodium-glucose co-transporter-2 inhibitors versus other glucose-lowering drugs (CVD-REAL Nordic): A multinational observational analysis. *Lancet Diabetes Endocrinol*. 2017;5:709–17.